

Journal Pre-proof

Investigation of physiological stress shielding within lumbar spinal tissue as a contributor to unilateral low back pain: a finite element study

Emily Newell, Mark Driscoll



PII: S0010-4825(21)00145-1

DOI: <https://doi.org/10.1016/j.combiomed.2021.104351>

Reference: CBM 104351

To appear in: *Computers in Biology and Medicine*

Received Date: 19 January 2021

Revised Date: 17 March 2021

Accepted Date: 17 March 2021

Please cite this article as: E. Newell, M. Driscoll, Investigation of physiological stress shielding within lumbar spinal tissue as a contributor to unilateral low back pain: a finite element study, *Computers in Biology and Medicine*, <https://doi.org/10.1016/j.combiomed.2021.104351>.

This is a PDF file of an article that has undergone enhancements after acceptance, such as the addition of a cover page and metadata, and formatting for readability, but it is not yet the definitive version of record. This version will undergo additional copyediting, typesetting and review before it is published in its final form, but we are providing this version to give early visibility of the article. Please note that, during the production process, errors may be discovered which could affect the content, and all legal disclaimers that apply to the journal pertain.

© 2021 Elsevier Ltd. All rights reserved.

Title Page

Title: Investigation of physiological stress shielding within lumbar spinal tissue as a contributor to unilateral low back pain: a finite element study

Authors: Emily Newell^a, Mark Driscoll^a

^a Musculoskeletal Biomechanics Research Lab, Department of Mechanical Engineering, McGill University, 845 Sherbrooke St. W, Montréal, Quebec, Canada, H3A 0G4

Author Emails: emily.e.newell@mail.mcgill.ca; mark.driscoll@mcgill.ca

Corresponding Author: Mark Driscoll

E-mail Address: mark.driscoll@mcgill.ca

Telephone: +1 (514) 398-6299

Fax: +1 (514) 398-7365

Abstract

Introduction The pathomechanism of low back pain (LBP) remains unknown. Unilateral LBP patients have demonstrated ipsilateral morphological and material property changes within the lumbar soft tissues, potentially leading to asymmetric tissue loading. Through the comparison of healthy and unilateral LBP validated finite element models (FEMs), this study investigates potential stress shielding consequential of spinal tissue property augmentation.

Methods Two FEMs of the musculoskeletal system – one demonstrating healthy and unilateral LBP conditions – were developed undergoing 30-degree flexion. FEMs included the vertebrae, intervertebral discs, and soft tissues from L1-S1. Material properties selected for the soft tissues were retrieved from published literature. To reflect unilateral LBP, the paraspinal morphology was atrophied, while the tissue moduli were increased. The symptomatic thoracolumbar fascia (TLF) was uniformly increased. Validation of the models preceded testing.

Results Model validation in spinal flexion was accomplished through comparison to literature. Compared to the healthy model, the unilateral LBP multifidus (MF), longissimus thoracis (LT), and TLF exhibited average tension changes of +7.9, -5.1, and +9.3%, respectively. Likewise, the symptomatic MF, LT, and TLF exhibited tension changes of +19.0, -10.4, and +16.1% respectively, whereas the asymptomatic MF, LT, and TLF exhibited -4.0, -2.0, and +0.4% changes in tension, respectively.

Conclusion Relative to the healthy tissues, the symptomatic LBP soft tissues demonstrated a 19.5 kPa increase in stress, with 99.8% of this increase distributed towards the TLF, suggesting a load allocation bias within the symptomatic unilateral LBP tissues. Consequentially, symptomatic paraspinal muscles may be unable to withstand loading, leading to stress shielding.

Keywords: Finite element analysis, physiological stress shielding, low back pain, biomechanics, thoracolumbar fascia, tissue mechanics, musculoskeletal system

Manuscript

Introduction

Low back pain (LBP) is one of the world's leading cause of disability [1]. Nearly 85% of people will experience LBP at least once within their lifetime [2], and yet upwards of 95% of cases are idiopathic [3, 4]. The majority of chronic, non-specific LBP sufferers have demonstrated poor recovery rates 12 months after the condition's onset [5, 6]. While interventions available to help manage pain and disabilities, such as pharmaceuticals and manual therapies, no conclusive treatment exists to cure long-term, non-specific LBP [7].

Researchers have focused considerably on the paraspinal muscles when investigating a potential pathomechanism of LBP. Clinical evidence has demonstrated abnormal tissue property augmentation in the soft tissues of LBP patients, with atrophy [8–15], fatty infiltration [14, 16], and increased modulus [17] of the lumbar muscles being commonly affiliated with LBP. Likewise, fascial tissue involved in force transmission has exhibits abnormal growth [18, 19] and reduced shear strain [19] in those experiencing LBP. Atrophy of the paraspinal muscles may be selective, with unilateral LBP patients often demonstrating atrophy in tissues on the symptomatic, or ipsilateral, side [12, 13, 15, 20, 21]. However, selective atrophy of the paraspinals may be a consequence of force imbalances, where inhibition of the paraspinal muscles on the symptomatic side may yield compensatory hypertrophy of asymptomatic paraspinals [12]. Scoliotic patients have likewise exhibited paraspinal asymmetry in which tissues of the concave side demonstrated significant degeneration relative to the convex side [22–26], paired with reduced muscle activity of concave soft tissues [23]. The asymmetry of tissues found within scoliotic spines may promote abnormal loading of the spinal tissues, yielding diminished muscle activity and increased muscle atrophy, leading to further asymmetric tissue degeneration and the progression of scoliotic deformation [22, 27, 28]. Continual tissue degeneration due to abnormal loading, followed by

irregular tissue activation, force balances, and tissue remodelling, may be indicative of cyclical stress shielding – a phenomenon previously demonstrated within scoliotic vertebral columns [29].

Physiological stress shielding, as defined by Driscoll et al. [30], occurs when strong tissues (i.e. those with higher rigidity) withstand the majority of a load – or stress – induced from physiological motion. In turn, weaker tissues are prevented from receiving normal loading. As stress acting on tissues acts as a trigger for mechanotransduction, the ability for the tissues to regulate their performance is altered. Stimuli-deficient tissues undergo degenerative tissue remodelling, leading to atrophy and reduced rigidity. These weakened tissues thus lose the ability to withstand normal loading. Conversely, excessively stimulated tissues yield maladaptive hypertrophy and increased tissue strength. Although this sequence of events has been commonly characterized in bone tissue through Wolff's Law [31], physiological stress shielding may have dire consequences on the soft tissues of the musculoskeletal system. Analogous to scoliotic spines, the lumbar paraspinals of unilateral LBP patients demonstrate asymmetric atrophy [12, 13]. Thus, loading of the asymmetric spinal tissues may produce the same sequence of irregular force balances and muscle activation as suggested within scoliotic tissues, possibly laying the foundation for cyclical stress shielding. Given the paraspinals' role in spinal stability, and the TLF's ability to transmit and withstand stress, augmentation of the soft tissues may compromise the ability for the tissues to aid in spinal stability [32].

Finite element method, a numerical method originally conceived for solving complex structural mechanics, has become a popular medium for conducting analysis in physiological and medical applications. Advancements in computational power have allowed for finite element analysis (FEA) to evaluate increasingly complex models of anatomical systems (e.g. the vertebral column) [33]. When applied to the medical field, FEA has yielded numerous benefits, allowing for physiological stress analysis (non-invasive, allows for the reconstruction of complex geometries and

loading conditions [34]), and medical device design (reduction in cost and time associated with device design performance testing, bench-testing, and prototyping [35]), and elimination of ethical concerns associated with *in vitro* or *in vivo* clinical studies [36]. The application of FEA in spine research has also provided an avenue for the assessment of spinal conditions, including analysis of the healthy spine, as well as altered spinal states consequential of degenerative conditions [33]. For *in silico* models to provide realistic representation of human anatomy and physiology, it is imperative that the models are validated through a comparison to *in vitro* (i.e. bench testing) or *in vivo* (i.e. clinical trials), allowing for the assessment of “the degree to which the computational model is an appropriate representation of the reality of interest” [37]. Thus, the objective of this study is to develop validated finite element models (FEMs) of the musculoskeletal system with healthy and unilateral LBP conditions to assess stress distributions to investigate the potential for physiological stress shielding in LBP.

Methods

To analyze the potential for stress shielding within spinal tissues affected by unilateral LBP, two FEMs depicting the lumbar musculoskeletal system were constructed leveraging previously extensively validated works [38]: one reflective of a healthy spine and one reflecting unilateral LBP. To construct FEMs reflective of realistic lumbar musculoskeletal tissue, CAD files of anatomical segments were obtained through 3DBodyParts/Anatomography, an open-source database. The volumetric CAD files available through 3DBodyParts/Anatomography were created from the parametric data extracted from MRIs of a healthy adult male, capturing anatomical segments’ morphological and geometric characteristics [39]. Models included the vertebrae, intervertebral discs (IVDs), lumbar muscles (i.e. the longissimus thoracis (LT), and multifidus (MF)) and their respective tendons, and the thoracolumbar fascia (TLF) from L1-S1. The obtained tissue geometries were subsequently processed into CAD files and imported into SpaceClaim

(V19.1, Concord, Massachusetts; Figure 1) to construct the models. As the FEMs sought to depict only the lumbar musculoskeletal system, soft tissues extending past the superior surface of L1 were bifurcated using an axial plane located 10mm above the L1 vertebra and subsequently removed.

Construction of a Healthy Model

Construction of the healthy model involved modelling the vertebrae, IVDs, tendons, LT, MF, and TLF as 3D volumetric bodies. Tissues were assumed to be homogenous, linear isotropic and near incompressible. Material properties of the tissues were obtained from literature [40–45] (Table 1). To represent near-incompressibility, tissues were assigned a Poisson's ratio of 0.45. The vertebrae, however, were assigned a Poisson's ratio of 0.3 [40]. Tissues were subsequently imported into ANSYS Static Structural (V19.1, Canonsburg, Pennsylvania) to undergo loading to assess soft tissue stress distributions.

Construction of a Unilateral LBP Model

The aforementioned healthy model was used as a reference for the construction of the unilateral LBP model. Similar to the healthy model, the unilateral LBP model was constructed using identical 3D volumetric bodies of the vertebrae, IVDs, tendons, LT, MF, and TLF. Tissues located laterally to the left and right of the vertebral column represented the “asymptomatic” and “symptomatic” soft tissues of unilateral LBP patients, respectively. The L4/L5 vertebral level was designated as the “peak” pain location of the unilateral LBP. To represent unilateral LBP patients' musculoskeletal systems, the cross-sectional areas (CSAs) and material properties of the symptomatic MF, LT, and TLF were modified, reflecting clinical findings involving unilateral LBP patients. The CSAs of the MF and LT were reduced incrementally at each vertebral level (Table 2). Reduction of the MF and LT at each vertebral level of the symptomatic tissues was calculated relative to the asymptomatic tissues to replicate the atrophy in CSA exhibited by MRIs of unilateral LBP patients as aggregated by Ploumis et al [13]. The symptomatic TLF was uniformly increased

across all vertebral levels, as per clinical data of LBP patients [18]. The moduli of the MF and LT were increased by 16.7% and 5.7%, respectively [17, 44] (Table 1). The unilateral LBP model was subsequently imported into ANSYS Static Structural to undergo loading. Only the aforementioned changes in tissue material properties and CSA differ between the two models.

Loading Scenario

Both FEMs underwent a loading scenario to induce 30-degree flexion by means of reproducing realistic loading experienced by the musculoskeletal system during physiological motion. As the paraspinal muscles contribute to spinal stabilization during flexion, the selected motion provides an ideal loading scenario for stress distribution analysis between healthy and LBP musculoskeletal soft tissues. To induce 30-degree flexion within the models, a 1175N compressive follower load was applied, in combination with a pure bending moment of 7.5Nm acting at the centroid of the L1 vertebral body (Figure 2) [46]. The tail of S1 was considered a fixed support. As no loading was placed on the soft tissues of both models, responses to loading by the soft tissues were passive. All connections between tissues were bonded. Contacts between soft tissues were considered frictionless to prevent the production of frictional stresses on the tissues.

Evaluation of Results and Validation

To investigate possible stress distribution discrepancies within healthy and unilateral LBP spinal tissues, the average tensile stress exhibited by the soft tissues in the longitudinal direction (+Z direction, Figure 1 coordinate system) was calculated. Through ANSYS Static Structural, the normal stress in the +Z direction was measured for each soft tissue at individual nodes. Results of the normal stress was then exported to MATLAB R2018b (MathWorks Inc., Natick, Massachusetts). Artifact nodes reporting compressive stress (≤ 0 Pa) were removed from the tabulated results, with the remaining nodes exhibiting tension being subsequently averaged. The process for calculating the average tension was conducted individually for the MF, LT, and TLF, in

both the healthy and unilateral LBP FEMs. For comparison of stress distributions in the symptomatic and asymptomatic tissues, this process was repeated for individual soft tissues located laterally to the left (i.e. asymptomatic) and right (i.e. symptomatic) of the vertebral column in the healthy and LBP FEMs.

To ensure the realistic representation of physiological motion of healthy and LBP spinal conditions, the IVD pressure and intervertebral rotation were calculated for both FEMs for the purpose of model validation. The maximum compression of each IVD was measured at the centre of each disc in both FEMs. Following this, the intervertebral rotation for each vertebra (L1-S1) was calculated using two reference markers. The first reference point was allocated to the centre of the posterior surface of the vertebral body, with the second located at a posteroinferior point on the inferior vertebra. Measured at the unflexed (0 degree, or initial position) and flexed (30-degree) positions, each vertebral translation in the anterior-posterior and inferior-superior directions was measured using the central vertebral point relative to the reference point in the inferior vertebra. Following the measurement of translational motion, changes in angular motion were calculated using MATLAB to determine the intervertebral rotation of each vertebra [47]. This process was repeated for each vertebral body in the healthy and unilateral LBP FEMs. The IVD pressure and intervertebral rotation of the healthy and unilateral LBP FEMs were compared to literature for validation purposes.

Sensitivity Analysis

The robustness of the models was evaluated through numerous sensitivity analyses. First, the mesh size of both models was modified from 3.0mm to 1.0mm using intervals of 0.5mm to evaluate the results' sensitivity to mesh sizing. A second sensitivity analysis involved varying the elastic moduli of the tendons to determine the models' sensitivity to the tendon material properties. Additionally, to determine the models' sensitivity to the vertebral material properties, the vertebral

bodies were treated as a composite material of cortical and cancellous bones with wide-ranging magnitudes of elastic moduli and Poisson's ratios. Lastly, the moduli of the LBP MF and LT were varied to determine the soft tissues' sensitivity to changes in the elastic modulus of each tissue.

Results

Twofold validation was accomplished through the comparison of the IVD pressure and intervertebral rotation of the healthy and unilateral LBP FEM lumbar vertebrae to literature. The IVD pressure of both FEMs was compared to the median IVD pressure of individually validated *in silico* lumbar spine models undergoing identical loading to induce flexion (Figure 3, "FEM Median") [36] and an *in vivo* study measuring L4/L5 IVD pressure during trunk flexion (Figure 3, "Wilke et al") [48]. The L4/L5 IVD pressure of the healthy and unilateral LBP FEMs each demonstrated a maximum deviation of 0.1 MPa relative to the L4/L5 IVD pressure as measured *in vivo* by Wilke et al [48]. Despite this minor deviation in IVD pressure relative to *in vivo* results, all IVD pressures measured by the healthy and unilateral LBP FEMs are within the "validated" range of IVD pressures obtained from the *in silico* models of the lumbar spine, as previously determined by Dreischarf et al [36]. Likewise, the models were validated by comparing the intervertebral rotation measured by the FEM lumbar vertebrae to the measured intervertebral rotation of patients undergoing 30-degree trunk flexion (Figure 4) [49]. Relative to the average intervertebral rotation for each lumbar vertebra as outlined by clinical data, the healthy and unilateral LBP FEMs exhibited a maximum deviation of 1.2 degrees in intervertebral rotation at the L1 vertebra (Figure 4, "Wong et al" [49]). Overall, the intervertebral rotation of the vertebrae composing the healthy and unilateral LBP FEMs are within the "acceptable" range of intervertebral rotation for 30-degree flexion as outlined by patient data (Figure 4) [49].

The unilateral LBP FEM demonstrated a minor decrease in the IVD pressure relative to the healthy FEM IVD at each IVD level, except for the L2/L3 IVD which demonstrated no change in

IVD pressure (Table 3). The maximum deviation in IVD pressure occurred at the L4/L5 IVD, with the unilateral LBP IVD demonstrating a decrease in compression by 6.9kPa (0.6%) relative to its healthy counterpart. For each of the vertebrae composing the unilateral LBP, there was no change in intervertebral rotation relative to the intervertebral rotation of the healthy FEM vertebrae. Results of the measured IVD pressure and intervertebral rotation at each vertebral level for the healthy and unilateral LBP FEMs are summarized in Table 3.

Despite undergoing identical loading, the unilateral LBP FEM soft tissues demonstrated significant differences in average soft tissue tension relative to the healthy FEM (Table 4). Overall, the LBP FEM soft tissues demonstrated an increase in tension from the healthy soft tissues by 10.94 kPa (9.24%). Compared to the healthy MF and LT, the LBP MF demonstrated elevated tension by 20.2 Pa (7.90%), while the LBP LT tension decreased by 1.2 Pa (5.11%). The largest difference in tension occurred within the TLF, with the LBP TLF undergoing a 10.92 kPa increase (9.24%) relative to the tension experienced by the healthy TLF.

In comparing the differences between soft tissue tension exhibited by the symptomatic and asymptomatic tissues (i.e. tissues located laterally right and left of the midline, respectively) relative to their healthy counterparts, the LBP FEM's symptomatic tissues exhibited a larger deviation in average tissue tension than the asymptomatic tissues (Table 4). Collectively, the LBP FEM's asymptomatic soft tissues increased in average tension relative to the healthy left lateral tissues by 0.49 kPa (0.42%). The LBP FEM's symptomatic soft tissues, however, increased overall by 19.52 kPa (16.10%). The LBP FEM's asymptomatic MF, LT, and TLF demonstrated changes in the average tension, with the MF and LT decreasing by 10.4 Pa (-3.99%) and 0.5 Pa (-2.00%) respectively and the TLF increasing by 0.5 kPa (0.43%) relative to the healthy tissues. The symptomatic LBP tissues, however, demonstrated larger discrepancies in individual soft tissue tension relative to the healthy tissues: the MF increased in tension by 47.9 Pa (18.99%) while the

LT decreased in tissue tension by 2.27 Pa (10.40%). The largest difference between the symptomatic tissues in the healthy and unilateral LBP FEM occurred in the TLF, with the LBP TLF increasing by 19.47 kPa (16.10%) from the healthy TLF.

Sensitivity analyses were conducted to demonstrate the validity of the assumptions used in the development of the FEMs, as well as the robustness of the aforementioned results obtained by both FEMs. Variation in mesh sizing demonstrated a maximum difference of < 12%. Variation in material properties of the tendon from the initial selection of elastic modulus yielded a < 5% deviation in results, indicating the models' robustness with respect to tendon properties. Modification to the material properties, including to treat the vertebrae as a composite of cancellous and cortical bone rather than a homogenous entity, resulted in a < 1% difference in results of IVD pressure. Furthermore, changes to soft tissue moduli yielded a maximum difference in LBP results for symptomatic tissues of < 14% when varying the elastic moduli of the LBP tissues. Despite the above impact on absolute values, the aforementioned relative comparisons between LBP and healthy hold true, giving confidence to the robustness of the model.

Discussion

Finite element analysis has become an increasingly popular method to non-invasively analyze the biomechanics of the human body. Often, analytical models seeking to investigate the biomechanics of the lumbar spine (or vertebral column) are osteoligamentous in design [36, 50–52]. Such models frequently utilize a follower load to provide an approximation of the compressive loading acting on the vertebral column during physiological motion [53]. In doing so, this also allows for the exclusion of volumetric skeletal muscles within the FEMs while still considering the contributions of local muscles to spinal stability during physiological loading on the spine [51, 54]. However, by excluding the volumetric bodies that represent muscles, such FEMs cannot consider the passive contributions of soft tissues to spine biomechanics. Moreover, the exclusion of the TLF

further neglects the passive contributions in which the fascia plays in spine biomechanics, including force transmission from the muscles to the vertebrae [55–58], and its influence on spinal stability and injury prevention during intersegmental motion [59]. The FEMs developed within this study sought to include the TLF, in addition to a follower load, to best capture the active and passive contributions of the musculoskeletal system. Additionally, many of the aforementioned *in silico* models portrayed and investigated the biomechanics of a healthy musculoskeletal system. As such, it is to the authors' knowledge that the FEM developed for this study is the first to investigate the effects of unilateral LBP on the musculoskeletal system relative to a healthy spine.

To objectively analyze the stress distributions of a musculoskeletal system in healthy and unilateral LBP conditions, both models were subjected to an identical, validated loading scenario to induce 30-degree flexion. To ensure an objective analysis, inter-subject variability in spinal profiles in both healthy and LBP spines had to be reduced. Therefore, the spinal profile of the LBP FEM was initially constructed by using the healthy spinal profile as its foundation. Only the material properties of its soft tissues were modified to accurately reflect LBP conditions [13, 17, 18]. As a result, the differences in stress distributions between the healthy FEM and the LBP FEM can only be attributed to said changes in tissue properties. As such, the potential for errors due to inter-subject variability was eliminated from the comparative analysis.

In relation to the healthy FEM, the IVDs of the unilateral LBP FEM demonstrated a decreasing trend in IVD pressure. While a negligible change in IVD pressure occurred at the L2/L3 IVD (0.01%), the largest discrepancy in IVD pressure between the FEMs was registered at the L4/L5 IVD (-0.58%). This trend in decreasing IVD pressure may indicate an abnormality in stress distributions within the vertebral column. It has been hypothesized that such irregularities may indicate the onset of IVD degeneration, with potential to cause discogenic pain [60]. While this may have some clinical implications regarding the spine's ability to withstand regular loading and

muscle activation patterns (due to unilateral LBP), further investigation is required to make this connection absolute.

Substantial discrepancies were observed when comparing the overall stress distributions between the healthy FEM and the unilateral LBP FEM. First, the unilateral LBP FEM demonstrated an average increase in cumulative tensile stress of 10.94 kPa (9.24%) relative to the healthy tissues. However, the majority of this 10.94 kPa stress increase was distributed towards the TLF (99.8%), with the MF and LT withstanding the remaining 0.2% of this increase in stress. While the LBP MF also demonstrated an increase in average tension from the healthy MF (7.90%), the LT exhibited a decrease in average tension relative to the healthy LT (-5.11%). Despite being a major contributor to spinal stability during flexion in a healthy spine, results suggest stress normally withstood by the LT may be redistributed towards the TLF. As such, this may indicate a reduction in normal loading for the LT, simultaneously increasing the stress acting on the TLF, signifying a potential load allocation bias. Furthermore, the increase in average tension, exhibited by the LBP soft tissues being skewed towards the TLF, may be a further indicator of a load allocation bias towards the TLF of unilateral LBP spines.

While the soft tissues of the unilateral LBP FEM demonstrated an overall increase in average tension compared to the soft tissues of the healthy FEM, this increase in average tension was not evenly distributed between the asymptomatic and symptomatic tissues. This asymmetric loading may be a consequence of the asymmetric muscle profile, which was implemented in the LBP FEM to reflect the musculature of unilateral LBP sufferers. For instance, while the asymptomatic soft tissues increased by 0.49 kPa (0.42%) relative to the healthy FEM tissues, the symptomatic soft tissues exhibited an increase in tension by 19.52 kPa (16.10%). It can be suggested, therefore, that the symptomatic tissues are bearing the brunt of the increased loading brought on by unilateral LBP.

Considering only the asymptomatic LBP tissues, the total average tension increased by 0.49 kPa (0.42%). However, the average tension of the asymptomatic LBP TLF increased by 0.5 kPa – a 104.2% increase relative to the overall increase in symptomatic tissues – while the average tension of the asymptomatic LBP MF and LT decreased by 10.4 Pa (-3.99%), and 0.5 Pa (-2.00%) respectively. Such changes in tissue tension show that the asymptomatic LBP TLF likely bears the load of the overall increase in stress across the asymptomatic tissues, in addition to the stress that would normally be withstood by the MF and LT in a healthy spine. This stress distribution pattern appears to be allocated towards the asymptomatic TLF, an outcome that is similar to the stress distribution demonstrated by the cumulative soft tissues of the LBP FEM relative to the healthy FEM.

Akin to the asymptomatic LBP soft tissues, the symptomatic LBP tissues experienced a greater increase in average soft tissue tension relative to the healthy soft tissues. However, the magnitude of the increase in tension experienced by the symptomatic tissues was remarkably larger than that experienced by the asymptomatic tissues. The overall average tension of the symptomatic LBP soft tissues increased by 19.52 kPa (16.10%) relative to the healthy tissues, of which 99.8% (19.47 kPa) was distributed towards the symptomatic TLF. The remaining 0.2% of the increase in tension was distributed towards the symptomatic LBP MF and LT. However, given the evident reduction in stress exhibited by the symptomatic LBP LT (-10.40%), it is likely that the symptomatic LBP MF is the predominant recipient of the remaining 0.2%. As the majority of the increased tension predominantly impacted the symptomatic LBP TLF, it can be ascertained that a load allocation bias exists within the symptomatic LBP tissues.

Discrepancies in the stress distributions between the healthy FEM and unilateral LBP FEM indicate a possible load allocation bias within the lumbar soft tissues of the LBP FEM. Notably, this load allocation bias is predominantly directed towards the TLF, which may be indicative of stress shielding, whereby the TLF withstands the majority of the stress increase following the onset of

unilateral LBP. In turn, the MF and LT receive reduced loading relative to healthy conditions. The reduction in loading may trigger atrophy through degenerative remodelling, reducing the ability for the MF and LT to withstand normal loading. To compensate, irregular muscle activation of alternative muscles may occur, leading to abnormal force balances acting on the soft tissues. As such, increased activation of these tissues undergoing larger-than-normal loading may lead to positive tissue remodelling. As LBP patients have demonstrated increased TLF morphology [18, 19], this further supports the notion of the TLF withstanding higher loading relative to a TLF in a healthy musculoskeletal system. Accordingly, this may lay the foundation for stress shielding within the lumbar soft tissues, whereby the TLF shields the paraspinal muscles from receiving loading. As a result, the MF and LT will further deteriorate, essentially trapping the paraspinals in a degenerative remodelling cycle. Given the vital contributions of the MF and LT to spinal stability, this degenerative sequence of events may be detrimental to the ability for the spine to be stabilized and withstand external loading [32]. As this iterative cycle is continuous, unless interrupted by the appropriate clinical intervention [30], long-term stress shielding within the lumbar soft tissues may contribute to the progression of LBP.

Analysis of the asymptomatic and symptomatic tissues reveals the effects of the muscle asymmetry with respect to the stress distributions of unilateral LBP. While the symptomatic and asymptomatic LBP tissues each demonstrated a load allocation bias towards the TLF, this bias was found to be more severe within the symptomatic tissues. For instance, the symptomatic LBP tissues demonstrate a 19 kPa difference in increased average tension relative to the asymptomatic LBP tissues, indicating asymmetric loading across the lumbar soft tissues of the LBP FEM. Given that the symptomatic LBP tissues are subjected to a greater change in average tension and larger discrepancies in stress distribution (i.e. relative to the asymptomatic LBP tissues), it is possible that the symptomatic LBP tissues are more susceptible to degenerative stress shielding. As previously discussed, the shielding of the symptomatic muscles by the TLF may result in the inability for the

MF and LT to withstand loading, eventually leading to an unconstrained cycle of further tissue degeneration, as well as irregular loading and tissue activation. This sequence of events may effectively trap the symptomatic tissues in a cycle of degenerative stress shielding.

Severe ipsilateral stress shielding may encourage the muscle asymmetry documented within unilateral LBP sufferers. For example, as demonstrated in scoliotic patients, loading of asymmetric spinal tissues leads to unbalanced tissue activation, yielding the atrophy of weaker, stimuli-deficient tissues. It has been suggested that this sequence of events promotes the muscle asymmetry within scoliotic spines and furthers the progression of the deformity instigated by scoliotic vertebral columns [22]. Furthermore, researchers have proposed that greater antagonistic muscle activation would be required to counteract the progression of spinal deformation associated with scoliosis [27]. Thus, asymmetric loading of the spinal tissues of unilateral LBP sufferers may be analogous to the asymmetric loading demonstrated within scoliotic spines. As such, the stress shielding within the symptomatic tissues may promote the spinal muscle asymmetry of unilateral LBP sufferers, potentially promoting stress shielding, and, in turn, LBP. Moreover, elevated muscle activity of the asymptomatic tissues may be required to counteract stress shielding within the symptomatic tissues. In turn, this may aid in the prevention of LBP progression within unilateral LBP spinal tissues. This, however, would require further investigation.

The FEMs developed for this study were indirectly validated by comparing the measured IVD pressure and intervertebral rotation to clinical and *in silico* data obtained from published literature. The results obtained from the healthy and LBP FEMs demonstrated good agreement with IVD pressure and intervertebral rotation data found in *in silico*, *in vivo*, and clinical studies [36, 48, 49]. The *in silico* data was retrieved from eight validated FEMs, with each model being constructed from unique patient-specific geometry and varied in material properties to represent the characteristics of biological tissues. Each of these *in silico* FEMs were previously validated individually, with the median values of results from these FEMs compared to *in vivo* data, resulting

in a range of “validated” IVD pressures for FEMs undergoing identical loading to induce flexion regardless of anatomical geometry and material properties used [36]. As such, the developed healthy and LBP FEMs measured IVD pressure within the “validated” range and can be considered indirectly validated. The L4/L5 IVD pressure results obtained from the healthy and LBP FEMs were additionally compared to *in vivo* data measured for the L4/L5 IVD, providing further validation of the models through *in vivo* studies [48]. Additionally, for intervertebral rotation at 30-degree flexion, the developed healthy and LBP FEMs were within the “validated” range as deemed acceptable by the clinical study [49]. Thus, the developed models may be considered validated, reaffirming the models’ validity in executing 30-degree flexion.

Limitations

To develop realistic *in silico* models depicting musculoskeletal systems in healthy and unilateral LBP conditions during physiological motion, multiple assumptions were required. First, both models were constructed using geometry obtained from an anatomographic database compiled from the MRIs of a young, adult Japanese male. Though *in vivo* studies may involve clinical patients, geometry of the musculoskeletal tissues can vary from subject to subject, introducing inter-subject variability in results obtained. Inter-subject variability can lead to difficulty in objectively determining the consequences of LBP on spine biomechanics relative to healthy spinal tissues. However, as each FEM was constructed using the same geometry to represent spinal tissues, inter-subject variability has been avoided. Additionally, the use of FEMs constructed from a male subject may not be conducive with the potential for stress shielding within biologically female sex as a result tissue property changes in LBP patients. As such, future studies are to include FEMs constructed from MRIs taken of subjects that are of the female sex. The inclusion of FEMs representative of all biological sexes will provide further insight into the potential for stress shielding within the lumbar spine to be universal, regardless of sex. Moreover, differences within the tissue stress distributions between healthy and LBP FEMs of different sexes may provide further

insight into the potential for and severity of stress shielding to occur within LBP patients of varying sex.

Additional assumptions included considering the vertebral bodies to be homogenous, rather than a composite material of cancellous and cortical bone tissue. Sensitivity analysis results demonstrated that the homogeneity of the vertebrae has little effect on the results measured from the FEMs. Additionally, all tissues within the FEMs were denoted as homogenous linear isotropic. Although biological tissues are inhomogeneous, viscoelastic, and anisotropic in nature, the material properties of the FEM tissues were obtained from previously validated *in silico* models or clinical trials. With respect to the soft tissues specifically, material properties were obtained through *in vivo* studies which involved the use of shear wave elastography – a methodology which estimates the shear modulus via ultrasound [17, 44]. Given the dependency on the shear wave velocity and the density of the skeletal tissue, the shear modulus may be estimated regardless of the tissue cross-section. Further, the elastic modulus can be subsequently determined through Hooke's law for isotropic materials ($E = 2G(1+\nu) \approx 3G$ for incompressible materials), providing realistic, passive behaviour of specific skeletal muscles in healthy subjects and LBP patients irrespective of tissue cross-section. Moreover, the sensitivity analysis varying the tissue moduli of the symptomatic MF and LT demonstrated a maximum difference $< 14\%$ for the symptomatic MF and $< 10\%$ for LT, indicating the results of the symptomatic tissues are relatively unaffected by changes in the modulus, regardless of the increased modulus of the symptomatic LBP MF and LT irrespective of the tissues' cross-section. Lastly, the stress distributions of the models' soft tissues outlined in this study were analyzed statically. Although tissues are viscoelastic, the static analysis of the stress distributions negates the effects of time on tissue behaviour. Future studies using dynamic analysis of the stress distributions changes in healthy and LBP should consider the use of viscoelastic effects on tissue behaviour.

The material properties of the tendons were unable to be determined from literature involving human subjects. The tendons' material properties were varied in a sensitivity analysis, with the FEMs demonstrating little deviance in the results obtained due to tendon properties. Overall, the FEMs demonstrated good validation in IVD pressure and intervertebral rotation. As validation for IVD pressure was achieved through the comparison to multiple validated *in silico* models with varying material properties, including nonlinear, anisotropic, and hyper-elastic properties undergoing an identical loading scenario [36], as well as comparison to *in vivo* IVD pressures [48], the use of linear elasticity for the healthy and unilateral LBP models may be considered acceptable. Furthermore, the simplification of material properties within the FEMs allowed for the reduction in computational cost and time, while ensuring the accuracy of the results of obtained by the model were not hindered. Finally, a mesh of 3mm was selected for the developed FEMs. However, mesh sensitivity analyses concluded results obtained were unaffected by mesh size. Thus, given the aforementioned assumptions for the construction of the FEMs, the FEMs may be considered robust.

Conclusion

This *in silico* study sought to comparatively analyze the stress distributions within the musculoskeletal system in healthy and unilateral LBP conditions as a means of determining the potential for stress shielding within the soft tissues as a contributor to the progression of LBP. Results demonstrated an overall increase in tension of the unilateral LBP tissues, with most of this stress increase being distributed towards the TLF. The majority of the load increase was skewed towards the symptomatic LBP tissues, indicating unbalanced loading as a result of asymmetric tissue properties. Asymmetric loading, paired with elevated stress within the symptomatic tissues directed towards the symptomatic LBP TLF, is notably absent within the healthy FEM. As a result, this load allocation bias within the symptomatic LBP tissues may be indicative of physiological stress shielding within unilateral LBP patients.

References

- [1] C. J. L. Murray, T. Vos, R. Lozano, M. Naghavi, A. D. Flaxman, C. Michaud, *et al.*, “Disability-adjusted life years (DALYs) for 291 diseases and injuries in 21 regions, 1990-2010: A systematic analysis for the Global Burden of Disease Study 2010,” *The Lancet*, vol. 380, no. 9859, pp. 2197–2223, 2012.
- [2] G. B. J. Andersson, “Epidemiological features of chronic low-back pain,” *The Lancet*, vol. 354, no. 9178, pp. 581–585, Aug. 1999.
- [3] R. A. Deyo and J. N. Weinstein, “Low back pain,” *N. Engl. J. Med.*, vol. 344, no. 5, pp. 363–370, 2001.
- [4] M. Lima, A. S. Ferreira, F. J. J. Reis, V. Paes, and N. Meziat-Filho, “Chronic low back pain and back muscle activity during functional tasks,” *Gait Posture*, vol. 61, pp. 250–256, 2018.
- [5] C. J. Itz, J. W. Geurts, M. Van Kleef, and P. Nelemans, “Clinical course of non-specific low back pain: A systematic review of prospective cohort studies set in primary care,” *Eur. J. Pain (United Kingdom)*, vol. 17, no. 1, pp. 5–15, 2013.
- [6] L. Costa, C. G. Maher, J. H. McAuley, M. J. Hancock, R. D. Herbert, K. M. Refshauge, *et al.*, “Prognosis for patients with chronic low back pain: Inception cohort study,” *Br. Med. J. (Clinical Res. Ed.)*, vol. 339, no. 7725, p. 850, 2009.
- [7] C. Maher, M. Underwood, and R. Buchbinder, “Non-specific low back pain,” *The Lancet*, vol. 389, no. 10070. Lancet Publishing Group, pp. 736–747, 18-Feb-2017.
- [8] M. Kamaz, D. Kireşi, H. Oğuz, D. Emlik, and F. Levendoğlu, “CT measurement of trunk muscle areas in patients with chronic low back pain,” *Diagn. Interv. Radiol.*, vol. 13, no. 3, pp. 144–148, 2007.
- [9] T. L. Wallwork, W. R. Stanton, M. Freke, and J. A. Hides, “The effect of chronic low back pain on size and contraction of the lumbar multifidus muscle,” *Man. Ther.*, vol. 14, no. 5, pp.

- 496–500, 2009.
- [10] L. A. Danneels, G. G. Vanderstraeten, D. C. Cambier, E. E. Witvrouw, and H. J. De Cuyper, “CT imaging of trunk muscles in chronic low back pain patients and healthy control subjects,” *Eur. Spine J.*, vol. 9, pp. 266–272, 2000.
- [11] J. Hides, W. Stanton, S. McMahon, K. Sims, and C. Richardson, “Effect of stabilization training on multifidus muscle cross-sectional area among young elite cricketers with low back pain,” *J. Orthop. Sport. Phys. Ther.*, vol. 38, no. 3, pp. 101–108, 2008.
- [12] Q. Wan, C. Lin, X. Li, W. Zeng, and C. Ma, “MRI assessment of paraspinal muscles in patients with acute and chronic unilateral low back pain,” *Br. J. Radiol.*, vol. 88, no. 1053, 2015.
- [13] A. Ploumis, N. Michailidis, P. Christodoulou, I. Kalaitzoglou, G. Gouvas, and A. Beris, “Ipsilateral atrophy of paraspinal and psoas muscle in unilateral back pain patients with monosegmental degenerative disc disease,” *Br. J. Radiol.*, vol. 84, no. 1004, pp. 709–713, 2011.
- [14] S. T. Chan, P. K. Fung, N. Y. Ng, T. L. Ngan, M. Y. Chong, C. N. Tang, *et al.*, “Dynamic changes of elasticity, cross-sectional area, and fat infiltration of multifidus at different postures in men with chronic low back pain,” *Spine*, vol. 12, no. 5, pp. 381–388, 2012.
- [15] K. L. Barker, D. R. Shamley, and D. Jackson, “Changes in the cross-sectional area of multifidus and psoas in patients with unilateral back pain: the relationship to pain and disability,” *Spine*, vol. 29, no. 22, pp. 515–519, 2004.
- [16] P. Kjaer, T. Bendix, J. S. Sorensen, L. Korsholm, and C. Leboeuf-Yde, “Are MRI-defined fat infiltrations in the multifidus muscles associated with low back pain?,” *BMC Med.*, vol. 5, no. 2, 2007.
- [17] M. Masaki, T. Aoyama, T. Murakami, K. Yanase, X. Ji, H. Tateuchi, *et al.*, “Association of low back pain with muscle stiffness and muscle mass of the lumbar back muscles, and

- sagittal spinal alignment in young and middle-aged medical workers,” *Clin. Biomech.*, vol. 49, pp. 128–133, Nov. 2017.
- [18] H. M. Langevin, D. Stevens-Tuttle, J. R. Fox, G. J. Badger, N. A. Bouffard, M. H. Krag, *et al.*, “Ultrasound evidence of altered lumbar connective tissue structure in human subjects with chronic low back pain,” *BMC Musculoskelet. Disord.*, vol. 10, no. 1, pp. 1–9, 2009.
- [19] H. M. Langevin, E. E. Konofagou, G. J. Badger, J. J. Triano, W.-N. Lee, J. R. Fox, *et al.*, “Reduced thoracolumbar fascia shear strain in human chronic low back pain,” *BMC Musculoskelet. Disord.*, vol. 12, no. 203, pp. 1–11, 2011.
- [20] M. J. Stokes, R. G. Cooper, G. Morris, and M. I. V. Jayson, “Selective changes in multifidus dimensions in patients with chronic low back pain,” *Eur. Spine J.*, vol. 1, no. 1, pp. 38–42, 1992.
- [21] D. F. Kader, D. Wardlaw, and F. W. Smith, “Correlation between the MRI changes in the lumbar multifidus muscles and leg pain,” *Clin. Radiol.*, vol. 55, no. 2, pp. 145–149, 2000.
- [22] N. Shafaq, A. Suzuki, A. Matsumura, H. Terai, H. Toyoda, H. Yasuda, *et al.*, “Asymmetric degeneration of paravertebral muscles in patients with degenerative lumbar scoliosis,” *Spine*, vol. 37, no. 16, pp. 1398–1406, 2012.
- [23] W. W. Lu, Y. Hu, K. D. K. Luk, K. M. C. Cheung, and J. C. Y. Leong, “Paraspinal muscle activities of patients with scoliosis after spine fusion: An electromyographic study,” *Spine*, vol. 27, no. 11, pp. 1180–1185, 2002.
- [24] K. A. Zapata, S. S. Wang-Price, D. J. Sucato, and M. Dempsey-Robertson, “Ultrasonographic Measurements of Paraspinal Muscle Thickness in Adolescent Idiopathic Scoliosis: A Comparison and Reliability Study,” *Pediatr. Phys. Ther.*, vol. 27, no. 2, pp. 119–125, 2015.
- [25] Y.-L. Chan, J. C. Y. Cheng, A. D. King, J. F. Griffith, and C. Metreweli, “MRI evaluation of multifidus muscles in adolescent idiopathic scoliosis,” *Pediatr. Radiol.*, no. 29, pp. 360–363,

1999.

- [26] G. Zoabli, P. A. Mathieu, and C. É. Aubin, “Back muscles biometry in adolescent idiopathic scoliosis,” *Spine*, vol. 7, no. 3, pp. 338–344, 2007.
- [27] I. A. F. Stokes and M. Gardner-Morse, “Muscle activation strategies and symmetry of spinal loading in the lumbar spine with scoliosis,” *Spine*, vol. 29, no. 19, pp. 2103–2107, 2004.
- [28] I. A. F. Stokes, H. Spence, D. D. Aronsson, and N. Kilmer, “Mechanical modulation of vertebral body growth,” *Spine*, vol. 21, no. 10, pp. 1162–1167, 1996.
- [29] M. Driscoll, C. E. Aubin, A. Moreau, I. Villemure, and S. Parent, “The role of spinal concave-convex biases in the progression of idiopathic scoliosis,” *Eur. Spine J.*, vol. 18, no. 2, pp. 180–187, 2009.
- [30] M. Driscoll and L. Blyum, “The presence of physiological stress shielding in the degenerative cycle of musculoskeletal disorders,” *J. Bodyw. Mov. Ther.*, vol. 15, no. 3, pp. 335–342, 2011.
- [31] J. Wolff, “Das Gesetz der Transformation der knochen.” Hirshwald, Berlin, 1892.
- [32] M. M. Panjabi, “The stabilizing system of the spine. Part I. Function, dysfunction, adaptation, and enhancement,” *J. Spinal Disord.*, vol. 5, no. 4, pp. 383–389, 1992.
- [33] M. J. Fagan, S. Julian, and A. M. Mohsen, “Finite element analysis in spine research,” *Proc. Inst. Mech. Eng. Part H J. Eng. Med.*, vol. 216, no. 5, pp. 281–298, 2002.
- [34] E. J. Rayfield, “Finite element analysis and understanding the biomechanics and evolution of living and fossil organisms,” *Annu. Rev. Earth Planet. Sci.*, vol. 35, pp. 541–576, 2007.
- [35] M. Driscoll, “The impact of the finite element method on medical device design,” *J. Med. Biol. Eng.*, vol. 39, no. 2, pp. 171–172, 2019.
- [36] M. Dreischarf, T. Zander, A. Shirazi-Adl, C. M. Puttlitz, C. J. Adam, C. S. Chen, *et al.*, “Comparison of eight published static finite element models of the intact lumbar spine: predictive power of models improves when combined together,” *J. Biomech.*, vol. 47, no. 8,

- pp. 1757–1766, 2014.
- [37] American Society of Mechanical Engineers, “Assessing credibility of computational modeling through verification and validation: application to medical devices,” American Society of Mechanical Engineers, New York, NY, USA, 2018.
- [38] I. El Bojairami, K. El Monajjed, and M. Driscoll, “Development and validation of a timely and representative finite element human spine model for biomechanical simulations,” *Sci. Rep.*, vol. 10, no. 21519, pp. 1–16, 2020.
- [39] N. Mitsuhashi, K. Fujieda, T. Tamura, S. Kawamoto, T. Takagi, and K. Okubo, “BodyParts3D: 3D structure database for anatomical concepts,” *Nucleic Acids Res.*, vol. 37, no. Database Issue, pp. D782–D785, 2009.
- [40] T. Smit, A. Odgaard, and E. Schneider, “Structure and function of vertebral trabecular bone,” *Spine*, vol. 22, no. 24, pp. 2823–2833, 1999.
- [41] H. Yang, S. Nawathe, A. J. Fields, and T. M. Keaveny, “Micromechanics of the human vertebral body for forward flexion,” *J. Biomech.*, vol. 45, no. 12, pp. 2142–2148, 2012.
- [42] K. A. Bonilla, A. M. Pardes, B. R. Freedman, and L. J. Soslowsky, “Supraspinatus tendons have different mechanical properties across sex,” *J. Biomech. Eng.*, vol. 141, no. 1, p. 011002, 2018.
- [43] L. H. Yahia, P. Pigeon, and E. A. DesRosiers, “Viscoelastic properties of the human lumbodorsal fascia,” *J. Biomed. Eng.*, vol. 15, no. 5, pp. 425–429, 1993.
- [44] M. Masaki, X. Ji, T. Yamauchi, H. Tateuchi, and N. Ichihashi, “Effects of the trunk position on muscle stiffness that reflects elongation of the lumbar erector spinae and multifidus muscles: an ultrasonic shear wave elastography study,” *Eur. J. Appl. Physiol.*, vol. 119, no. 5, pp. 1085–1091, Feb. 2019.
- [45] M. Creze, M. Soubeyrand, J. L. Yue, O. Gagey, X. Maître, and M. F. Bellin, “Magnetic resonance elastography of the lumbar back muscles: A preliminary study,” *Clin. Anat.*, vol.

- 31, no. 4, pp. 514–520, 2018.
- [46] A. Rohlmann, T. Zander, M. Rao, and G. Bergmann, “Realistic loading conditions for upper body bending,” *J. Biomech.*, vol. 42, no. 7, pp. 884–890, 2009.
- [47] R. M. Lin, C. Y. Yu, Z. J. Chang, and F. C. Su, “Flexion-extension rhythm in the lumbosacral spine,” *Spine*, vol. 19, no. 19, pp. 2204–2209, 1994.
- [48] H. Wilke, P. Neef, M. Caimi, T. Hoogland, and L. E. Claes, “New In Vivo Measurements of Pressures in the Intervertebral Disc in Daily Life,” *Spine*, vol. 24, no. 8, pp. 755–762, 1999.
- [49] K. W. N. Wong, J. C. Y. Leong, M. K. Chan, K. D. K. Luk, and W. W. Lu, “The flexion-extension profile of lumbar spine in 100 healthy volunteers,” *Spine*, vol. 29, no. 15, pp. 1636–1641, 2004.
- [50] J. Q. Campbell, D. J. Coombs, M. Rao, P. J. Rullkoetter, and A. J. Petrella, “Automated finite element meshing of the lumbar spine: Verification and validation with 18 specimen-specific models,” *J. Biomech.*, vol. 49, no. 13, pp. 2669–2676, Sep. 2016.
- [51] A. Rohlmann, H.-J. Wilke, L. Bauer, G. Bergmann, and T. Zander, “Determination of trunk muscle forces for flexion and extension by using a validated finite element model of the lumbar spine and measured in vivo data,” *J. Biomech.*, vol. 39, no. 6, pp. 981–989, 2005.
- [52] T. Zander, A. Rohlmann, J. Calisse, and G. Bergmann, “Estimation of muscle forces in the lumbar spine during upper-body inclination,” *Clin. Biomech.*, vol. 16, no. 1, pp. S73–S80, Jan. 2001.
- [53] A. G. Patwardhan, R. M. Havey, K. P. Meade, B. Lee, and B. Dunlap, “A follower load increases the load carrying capacity of the lumbar spine in compression,” *Spine*, vol. 24, no. 10, pp. 1003–1009, 1999.
- [54] A. Rohlmann, S. Neller, L. Claes, G. Bergmann, and H. J. Wilke, “Influence of a follower load on intradiscal pressure and intersegmental rotation of the lumbar spine.,” *Spine*, vol. 26, no. 24, pp. 557–561, 2001.

- [55] F. H. Willard, A. Vleeming, M. D. Schuenke, L. Danneels, and R. Schleip, "The thoracolumbar fascia: anatomy, function and clinical considerations," *J. Anat.*, vol. 221, no. 6, pp. 507–536, 2012.
- [56] P. J. Barker, C. A. Briggs, and G. Bogeski, "Tensile transmission across the lumbar fasciae in unembalmed cadavers: effects of tension to various muscular attachments," *Spine*, vol. 29, no. 2, pp. 129–138, 2004.
- [57] M. Driscoll, "Fascia – The unsung hero of spine biomechanics," *Journal of Bodywork and Movement Therapies*, vol. 22, no. 1, pp. 90–91, Jan-2018.
- [58] K. El-Monajjed and M. Driscoll, "A finite element analysis of the intra-abdominal pressure and paraspinal muscle compartment pressure interaction through the thoracolumbar fascia," *Comput. Methods Biomech. Biomed. Engin.*, vol. 23, no. 10, pp. 585–596, 2020.
- [59] P. J. Barker and C. A. Briggs, "Anatomy and biomechanics of the lumbar fasciae: implications for lumbopelvic control and clinical practice," in *Movement, Stability & Lumbopelvic Pain: Integration of Research and Therapy*, 2nd ed., A. Vleeming, V. Mooney, and R. Stoeckart, Eds. London, UK: Elsevier Inc., 2007, pp. 63–73.
- [60] M. A. Adams, D. S. McNally, and P. Dolan, "'Stress' distributions inside intervertebral discs," *J. Bone Jt. Surg.*, vol. 78, no. 6, pp. 965–972, 1996.

Funding Information

This work was supported by the Natural Sciences and Engineering Research Council (NSERC) [grant no. NSERC GP514085-17] and the Fonds de Recherche du Québec – Nature et Technologies (FRQNT) [grant no. NC - 205220].

Figures

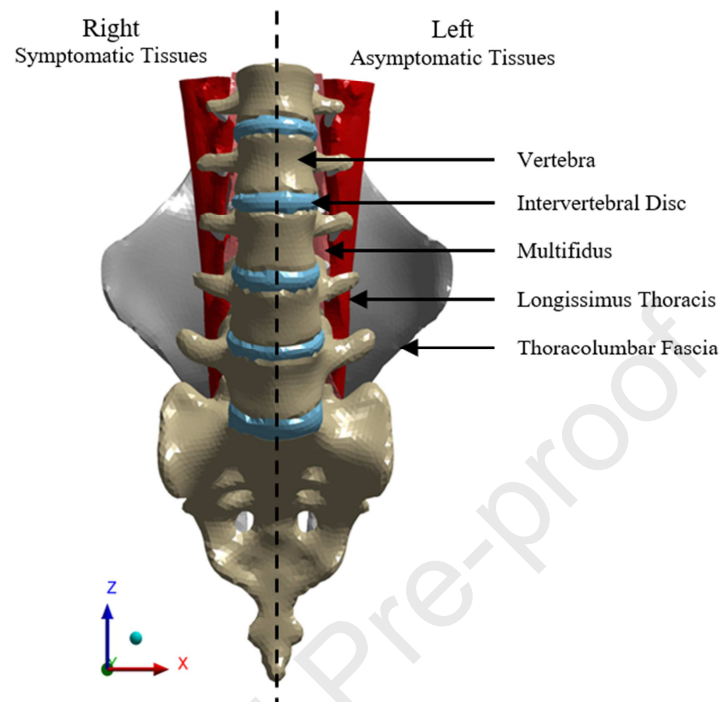


Fig. 1. Anatomy included within the finite element models. Finite element model of the lumbar musculoskeletal system demonstrating the vertebrae (L1-S1), intervertebral discs, and soft tissues (multifidus, longissimus thoracis, and thoracolumbar fascia). The unilateral low back pain model tissues are segregated through the midline of the vertebral column (given by the dashed line), with the material properties of tissues located to the right of the midline (“symptomatic”) are augmented to reflect unilateral low back pain patients. **This is a single column fitting image.**

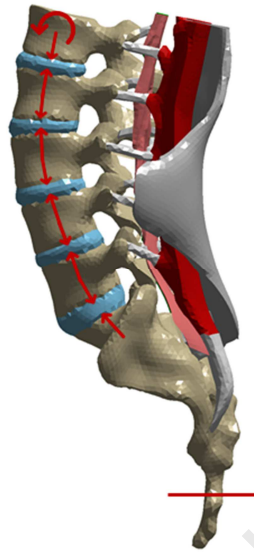


Fig. 2. Loading scenario acting on the developed finite element models. Loading scenario of the finite element models to induce 30-degree flexion, involving a 1175 N follower load acting at the centre of each vertebral body towards the adjacent vertebral body central and a 7.5 Nm acting at the L1 centroid (denoted by red arrows). The tail of S1 acted as a fixed support. **This is a one-column fitting figure.**

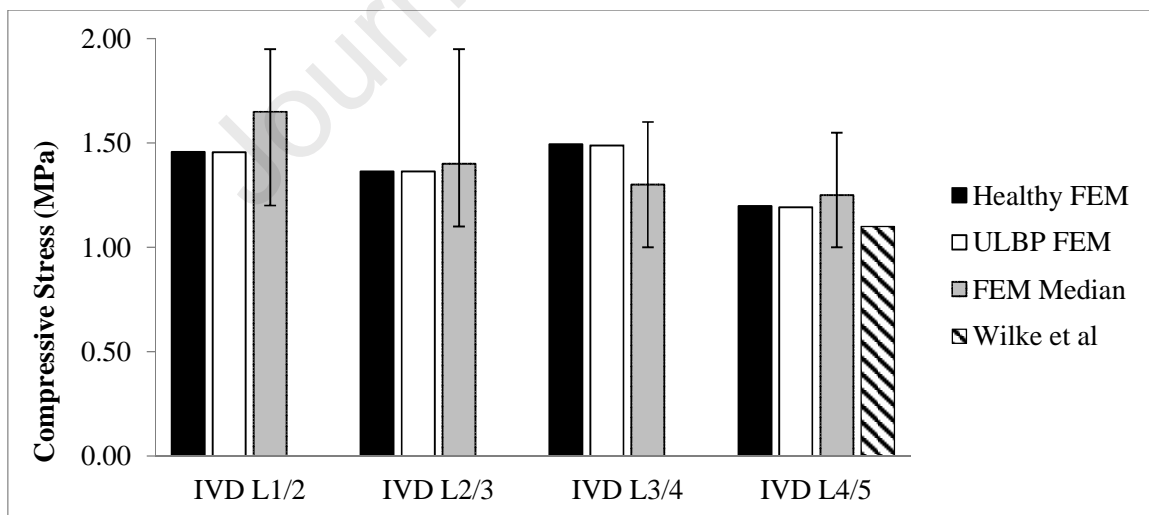


Fig. 3. Title: Intradiscal pressure of the lumbar vertebrae undergoing trunk flexion. Measured pressure of the intervertebral disc (IVD) for the lumbar IVDs for the unilateral low back pain (ILBP) and healthy finite element models (FEMs) in comparison to IVD pressure measured *in vivo* at L4/L5 during trunk flexion

(“Wilke et al”) [48] and the median IVD pressure exhibited by previously validated *in silico* models (“FEM Median”) [36]. Error bars indicate the range of IVD pressures obtained from the *in silico* FEMs [36]. **This is a 1-column fitting figure.**

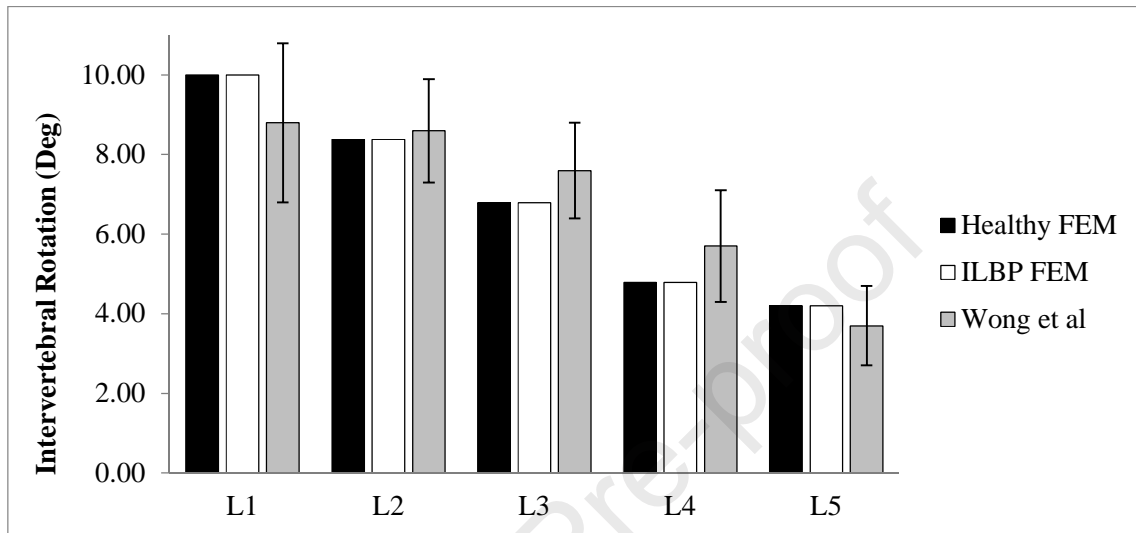


Fig. 4. Title: Intervertebral rotation of lumbar vertebrae undergoing 30° trunk flexion. Intervertebral rotation of the vertebrae of the healthy and unilateral low back pain (ULBP) finite element models (FEMs) in comparison to clinical studies involving 30 degree trunk flexion of patients in the sagittal plane [49]. **This is a 1-column fitting figure.**

Tables

Tissue	Young's Modulus (MPa)			Poisson's Ratio (Unitless)		
	Healthy FEM	LBP FEM	% Diff.	Healthy FEM	LBP FEM	% Diff.
Vertebrae	3000	3000	-	0.30	0.30	-
Intervertebral Discs	8	8	-	0.45	0.45	-
Tendons	200	200	-	0.45	0.45	-
Multifidus	0.092	0.107	16.7%	0.45	0.45	-
Longissimus Thoracis	0.041	0.043	5.7%	0.45	0.45	-
Thoracolumbar Fascia	416.67	416.67	-	0.45	0.45	-

Table 1 Material properties of tissues composing the healthy and unilateral low back pain (LBP) finite element models (FEMs) [17, 40–45].

Vertebral Level	Tissue Cross-Sectional Area		
	Multifidus	Longissimus Thoracis	Fascia
L1/L2	↓ 18.1%	↓ 0.2%	
L2/L3	↓ 15.6%	↓ 5.6%	
L3/L4	↓ 13.1%	↓ 11.0%	↑ 32.7%
L4/L5	↓ 10.7%	↓ 16.3%	
L5/S1	↓ 8.1%	↓ 21.8%	

Table 2 Change in cross-sectional area of the symptomatic tissues relative to the asymptomatic tissues at each intervertebral level for the low back pain (LBP) finite element model (FEM). The thoracolumbar fascia was increased uniformly across all vertebral levels.

	Healthy FEM	LBP FEM	% Difference
IVD Pressure (MPa)			
L1/L2	1.4572	1.4551	-0.14%
L2/L3	1.3636	1.3638	0.01%
L3/L4	1.4938	1.4892	-0.31%
L4/L5	1.1978	1.1909	-0.58%
L5/S1	1.0791	1.0774	-0.16%
Vertebral Rotation (deg)			
L1	9.9972	9.9972	-
L2	8.3811	8.3811	-
L3	6.7902	6.7902	-
L4	4.7841	4.7841	-
L5	4.2012	4.2012	-

Table 3 Measured intervertebral disc (IVD) pressures (in MPa) and intervertebral rotation (in degrees) of the healthy and low back pain (LBP) finite element models (FEMs).

Tissue	Symptomatic Tissues (kPa)			Asymptomatic Tissues (kPa)			Both Tissues (kPa)		
	Healthy	LBP	% Diff.	Healthy	LBP	% Diff.	Healthy	LBP	% Diff.
Multifidus	0.252	0.300	18.99%	0.259	0.249	-3.99%	0.256	0.276	7.90%
Longissimus Thoracis	0.0219	0.0196	-10.40%	0.0254	0.0249	-2.00%	0.0238	0.0226	-5.11%
Thoracolumbar Fascia	120.92	140.39	16.10%	115.33	115.83	0.43%	118.12	129.04	9.24%
Total	121.19	140.71	16.10%	115.62	116.10	0.42%	118.40	129.34	9.24%

Table 4 Measured normal stress (in kPa) of the symptomatic (right lateral), asymptomatic (left lateral), or both symptomatic and asymptomatic tissues in the longitudinal direction within the healthy and unilateral low back pain (ILBP) finite element models (FEMs).

Highlights

- Development of musculoskeletal models reflective of healthy and low back pain
- Analysis of stress distribution discrepancies between healthy and back pain models
- Pain model tissues increased by 19.5 kPa; 99.8% of increase skewed towards fascia
- Possible load allocation bias within pain model may be indicative of stress shielding

Journal Pre-proof

Conflict of Interest Statement

The authors of the manuscript, “Investigation of physiological stress shielding within lumbar spinal tissue as a contributor to unilateral low back pain: a finite element study”, Emily Newell and Dr. Mark Driscoll, declare that they have no conflict of interest.

Journal Pre-proof